

A Chemical Strategy for the Relaxivity Enhancement of Gd^{III} Chelates Anchored on Mesoporous Silica Nanoparticles

Fabio Carniato,^[a] Lorenzo Tei,^[b] Maurizio Cossi,^[a] Leonardo Marchese,^{*,[a]} and Mauro Botta^{*,[b]}

Abstract: Functionalised MCM-41 mesoporous silica nanoparticles were used as carriers of Gd^{III} complexes for the development of nanosized magnetic resonance imaging contrast agents. Three Gd^{III} complexes based on the 1,4,7,10-tetraazacyclododecane scaffold (DOTA; monoamide-, DOTA- and DO3A-like complexes) with distinct structural and magnetic properties were anchored on the silica nanoparticles functionalised with NH₂ groups. The interaction between Gd^{III} chelates and surface functional groups markedly influenced the relaxometric properties of the hybrid materials, and were deeply modified passing from ionic –NH₃⁺ to neutral amides. A complete study of the structural, textural and sur-

face properties together with a full ¹H relaxometric characterisation of these hybrid materials before and after surface modification was carried out. Particularly for the anionic complex **2** attached to MCM-41, an impressive increase in relaxivity (r_{1p}) was observed (from 20.3 to 37.8 mm^{−1}s^{−1}, 86.2% enhancement at 20 MHz and 310 K), mainly due to a threefold faster water exchange rate after acetylation of the surface –NH₃⁺ ions. This high r_{1p} value, coupled with the large molar amount of grafted **2** onto the silica

nanoparticles gives rise to a value of relaxivity per particle of 29 500 mm^{−1}s^{−1}, which possibly allows it to be used in molecular imaging procedures. Smaller changes were observed for the hybrid materials based on neutral **1** and **3** complexes. In fact, whereas **1** shows a weak interaction with the surface and acetylation induced only some decrease of the local rotation, complex **3** appears to be involved in a strong interaction with surface silanols. This results in the displacement of a coordinated water molecule and in a decrease of the accessibility of the solvent to the metal centre, which is unaffected by the modification of ammonium ions to neutral amides.

Keywords: gadolinium • imaging agents • mesoporous materials • nanostructures • relaxivity


Introduction

Magnetic resonance imaging (MRI) has rapidly gained a prominent role in diagnostic medicine for its ability to deliver three-dimensional images with superb spatial resolution.

However, MRI suffers from a relatively low sensitivity and in about 33% of examinations it requires the aid of exogenous species, contrast agents (CAs), to effectively image the anatomical details of interest. The use of highly efficient CAs is also essential in molecular imaging protocols, the development of which has recently been an object of great interest.^[1,2] The efficiency of a paramagnetic probe is partially described by its relaxivity, r_{1p} , which contains information on the structural, dynamic and electronic properties of the complex and on its magnetic coupling with the solvent molecules. There is active research aimed at enhancing the relaxivity through the optimisation of the relevant molecular relaxation parameters.^[2] The most important are the residence lifetime, τ_M , of the metal-coordinated water molecule(s) and the rotational motion of the paramagnetic system, described by the correlation time, τ_R . One approach to obtain highly efficient CAs is based on the conjugation of several gadolinium(III) complexes to polymers^[1] or dendrimers^[1] to increase the loading of active paramagnetic centres and, at

[a] Dr. F. Carniato, Prof. M. Cossi, Prof. L. Marchese
Dipartimento di Scienze e Tecnologie Avanzate
Centro Interdisciplinare Nano-Sistemi
Università del Piemonte Orientale "Amedeo Avogadro"
Viale T. Michel 11, 15121 Alessandria (Italy)
Fax: (+39) 0131-360250
E-mail: leonardo.marchese@mfn.unipmn.it

[b] Dr. L. Tei, Prof. M. Botta
Dipartimento di Scienze dell'Ambiente e della Vita
Università del Piemonte Orientale "Amedeo Avogadro"
Viale T. Michel 11, 15121 Alessandria (Italy)
Fax: (+39) 0131-360250
E-mail: mauro.botta@mfn.unipmn.it

 Supporting information for this article is available on the WWW under <http://dx.doi.org/10.1002/chem.201000499>.

the same time, to enhance the relaxivity per Gd as a consequence of the reduced global tumbling motion. In a different approach, but with similar results, the paramagnetic chelates are anchored or embedded on a number of nanosized systems (e.g., liposomes,^[3] virus capsids,^[4] zeolites,^[5] gold,^[6] silica^[7,8] or TiO₂^[9] nanoparticles).

Among these, mesoporous organosilica nanoparticles, because of their high versatility and biocompatibility, have been recently exploited for the development of MR-enhancing hybrid materials as Gd^{III}-complex carriers.^[10–13] However, in view of a possible use of these organosilica nanoparticles for in vivo experiments, a detailed investigation of their surface properties, in terms of reactivity and functionalisation degree, is required to understand the nature of the potential interactions with the biological tissues.

Recently, two novel hybrid materials based on different mesoporous silicas (SBA-15 and nanosized MCM-41) grafted with thermodynamically and kinetically stable DOTA-monoamide Gd complexes (H₄DOTA=1,4,7,10-tetraazacyclododecane-*N,N',N'',N'''*-tetraacetic acid) were prepared and investigated in our laboratories.^[7] This work showed that the mesoporous supports play a significant role in the physico-chemical properties of the final hybrid materials, as the distribution of the Gd^{III} complexes on the inner and/or outer surface was strictly dependent on the pore size and markedly influenced their relaxometric properties. More specifically, high longitudinal molar relaxivity was estimated for the materials functionalised with Gd^{III} complexes anchored on the external surface of the particles, due to a high accessibility of the water molecules to the paramagnetic centre.

These preliminary results stimulated further studies on the effects of the chemical nature of the organosilica surface on the magnetic properties of different Gd^{III} chelates immobilised on nanosized (20–50 nm) MCM-41 nanoparticles.^[14] For this reason, in addition to the neutral Gd–DOTA monoamide complex^[7] (**1**, Scheme 1), in which one water molecule occupies the first coordination sphere of the metal centre ($q=1$) with a τ_M of approximately 1 μ s at 298 K,^[15]

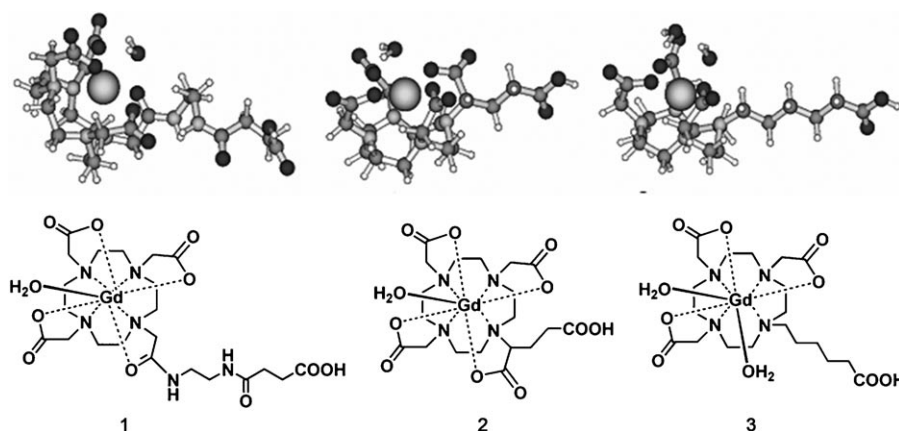
two Gd^{III} complexes with different structures and magnetic properties were selected for the functionalisation of the nanoparticle surface. One is the negatively charged Gd–DOTAGA (**2**, Scheme 1; DOTAGA=2-(*R*)-2-(4,7,10-triscarboxymethyl-1,4,7,10-tetraazacyclododec-1-yl)pentanedioic acid), which features four carboxylate donor groups and one inner-sphere water molecule with a sensibly shorter τ_M value (ca. 200 ns).^[16] The other is a neutral Gd–DO3A derivative (H₃DO3A=1,4,7,10-tetraazacyclododecane-1,4,7-triacetic acid) in which the metal ion can accommodate two water molecules ($q=2$) in the mon capped square-antiprismatic structure (**3**, Scheme 1).^[17] These q values are a reasonable assumption on the basis of the results obtained on a large number of related complexes.^[1]

Herein we report on the first example of a large modulation of the relaxivity of MCM-41 hybrid materials paramagnetically labelled with macrocyclic Gd complexes upon modification of the surface functional groups. The study is completed by the analysis of structural, textural, surface and ¹H relaxometric properties of these novel MR-enhanced systems.

Results and Discussion

Nanosized MCM-41 with particle sizes in the range 20–50 nm, as estimated by an average of more than a hundred crystals measured by TEM microscopy (Figure S1 in the Supporting Information), and pore diameters of approximately 25 Å^[14] was synthesised through a sol–gel procedure by using a block-copolymer and surfactant-assisted co-assembly method reported in the literature.^[14] The silanol-rich surface of the calcined support was activated by reaction with a suspension of aminopropyltriethoxysilane in toluene at 50 °C for 24 h.

MCM-41 nanoparticles were characterised by infrared spectroscopy before and after functionalisation with –NH₂ groups. The IR spectrum of nanosized MCM-41, collected at room temperature under vacuum, showed a band at 3745 cm^{–1} due to the stretching of isolated silanol groups (Si–OH) and a broad band in the 3700–3200 cm^{–1} range assigned to Si–OH groups involved in hydrogen bonds (Figure 1A, solid line). A drastic decrease of these absorptions was observed after reaction with aminopropyltriethoxysilane. In addition, new bands at 3370 and 3300 cm^{–1} (Figure 1A, dashed line) and 1595 cm^{–1} (Figure 1A', dashed line) assigned to the asymmetric and symmetric stretching and bending modes of NH₂, respectively, were observed in the NH₂/MCM-41



Scheme 1. GdL1 (**1**), GdL2 (**2**) and GdL3 (**3**) complexes. A molecular optimisation of the complexes is reported above each structure (see the Experimental Section for details of the computational analysis).

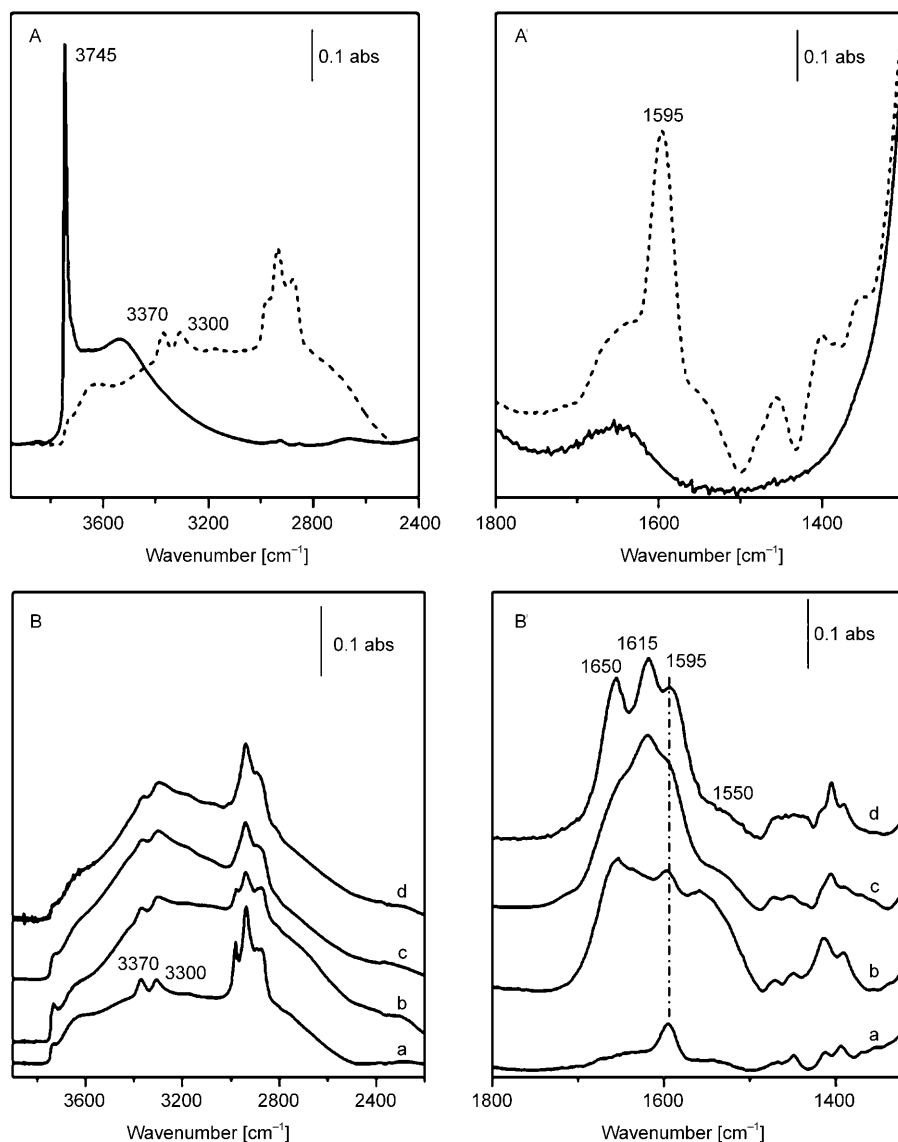


Figure 1. A), A') IR spectra, collected at RT and under vacuum, of nanosized MCM-41 (—) and NH₂/MCM-41 (----) outgassed at room temperature. IR spectra of a) NH₂/MCM-41, b) 1/MCM-41, c) 2/MCM-41 and d) 3/MCM-41 recorded at higher and lower frequencies are reported in parts B and B', respectively.

spectrum. These results suggested that a significant fraction of silanols were involved in the grafting reaction. Approximately 2.0 mmol g⁻¹ NH₂ groups (ca. 1.5 -NH₂ per nm²) were estimated to be in the final material by thermogravimetric analysis (Figure S2 in the Supporting Information).

The three ligands **L1**,^[7] **L2**^[18] and **L3**^[19] and the corresponding Gd^{III} complexes were synthesised by a slight modification of methodologies reported in the literature and is briefly described in the Experimental Section.

The complexes were anchored on the mesoporous nanoparticle surface by reaction between the free carboxylic group of the Gd^{III} chelates and the NH₂- functionalities present on both the internal and external silica surfaces of nanosized MCM-41. The reaction was carried out by stirring

for 24 h at room temperature a suspension in DMF, using *O*-(7-azabenzotriazol-1-yl)-*N,N,N',N'*-tetramethyluronium hexafluorophosphate (HATU) as an acid activator and *N,N*-diisopropylethylamine as a base. The final products were washed several times with water and dried at 50 °C for 3 h.

The amount of Gd in the final hybrid materials, 1/MCM-41, 2/MCM-41 and 3/MCM-41, was determined by inductively coupled plasma optical emission spectrometry (ICP-OES) measurements to be 0.050 (360 complex 1 molecules per particle), 0.119 (780 complex 2 molecules per particle) and 0.036 mmol g⁻¹ (240 complex 3 molecules per particle), respectively.

IR spectra of all the hybrid materials evidenced the presence of two bands at 1650 and 1550 cm⁻¹ due to the stretching and bending of the CO and NH of the amide groups, respectively, formed in the anchoring reaction (Figure 1B and B'). All spectra also displayed bands of amino groups (3370, 3300 and 1595 cm⁻¹) suggesting that a significant amount of these species was not involved in the reaction with the complexes (Figure 1B and B').^[19] Nevertheless, the intensities of NH₂ absorptions were weaker for 2/MCM-41 than for the other hybrid solids, in agreement with the presence of a larger concentra-

tion of anchored Gd^{III} complexes.

X-ray profiles of 1/MCM-41, 2/MCM-41 and 3/MCM-41 were collected and compared with the X-ray diffraction pattern of nanosized MCM-41 and NH₂/MCM-41 (Figure 2). MCM-41 (Figure 2a) showed three distinct reflections: one intense peak at 2θ = 2.3° and two weak reflections at 2θ = 4.0 and 4.7°, which are due to the (100), (110) and (200) planes, respectively, related to the hexagonal pore array of MCM-41.^[14] NH₂/MCM-41 and the GdL/MCM-41 hybrid materials displayed a decrease of the XRD peak intensity representing the presence of organic species (Figure 2b–e) with respect to pristine MCM-41 due to the modification of the scattering properties of the solids. However, structural order was preserved after the anchoring reactions, as high-

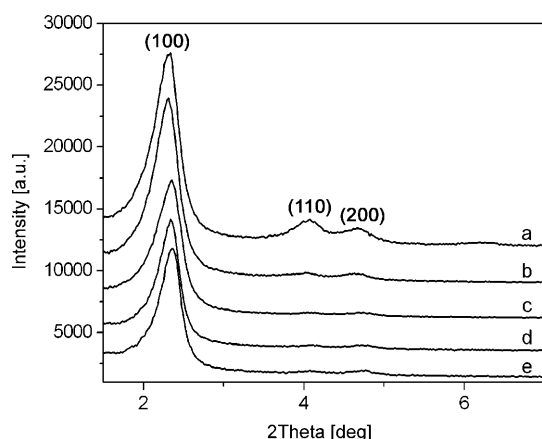


Figure 2. X-ray profiles of nanosized a) MCM-41, b) $\text{NH}_2/\text{MCM-41}$, c) **1**/MCM-41, d) **2**/MCM-41 and e) **3**/MCM-41.

lighted by the narrow and distinct XRD basal reflection (100).

Particular attention was also devoted to studying the textural properties of the final hybrid materials by nitrogen adsorption at 77 K, which allowed the Brunauer–Emmett–Teller surface area (S_{BET} in $\text{m}^2 \text{g}^{-1}$), volume (in $\text{cm}^3 \text{g}^{-1}$) and diameter (in Å) of the mesopores of the materials (Table 1) to be estimated. For pure nanosized MCM-41 and functionalised materials, the isotherms were type IV according to the IUPAC classification.

Table 1. Textural properties of mesoporous support and the hybrid materials.

	S_{BET} [$\text{m}^2 \text{g}^{-1}$]	Pore volume [$\text{cm}^3 \text{g}^{-1}$]	Pore diameter [Å]
MCM-41	890	0.71	25
$\text{NH}_2/\text{MCM-41}$	860	0.53	21
1 /MCM-41	624	0.40	21D
2 /MCM-41	540	0.35	19
3 /MCM-41	430	0.27	19

Nanosized MCM-41 synthesised in this work showed a surface area of $890 \text{ m}^2 \text{g}^{-1}$ and a pore diameter of 25 Å. The anchoring of NH_2 groups modified the final textural properties of the hybrid material leading to a significant decrease of the average pore diameter from 25 to 21 Å, thus confirming the presence of NH_2 groups inside the silica channels.

In the case of Gd^{III} -containing MCM-41, the pore-size distribution of the materials essentially retained its original mean value, which suggested that the complexes were anchored mainly on the external surface of the nanoparticles (Table 1 and Figure 3). However, in particular for **2**/MCM-41 and **3**/MCM-41, the mesopore volume drastically decreased in comparison to pristine $\text{NH}_2/\text{MCM-41}$, passing from 0.53 to 0.35 and $0.27 \text{ cm}^3 \text{g}^{-1}$, respectively, highlighting partial pore blocking.

These results are evidence of a different distribution of the Gd^{III} chelates on the external surface of MCM-41 nano-

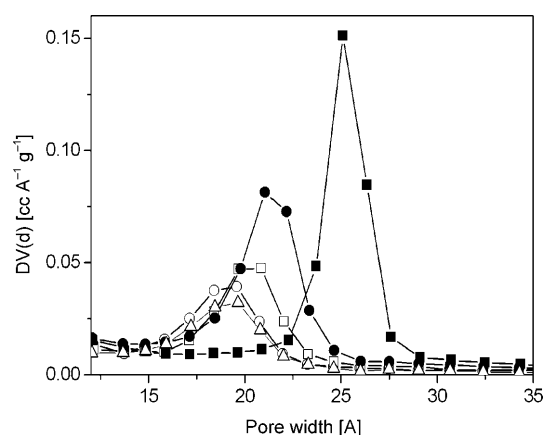


Figure 3. Pore-diameter distribution of nanosized MCM-41 (■), $\text{NH}_2/\text{MCM-41}$ (●), **1**/MCM-41 (□), **2**/MCM-41 (○), and **3**/MCM-41 (△).

particles, probably due to the different dimensions and molecular conformations of the complexes and their interaction with the silica surface. Since the pores play a prominent role in defining the overall surface area, the differences between the Gd content and the textural properties could be ascribed to the different distribution of the complexes between the external surface and the inner pores.

The proton longitudinal relaxivity, r_{1p} , of the hybrid materials was measured at 20 MHz and 310 K in aqueous suspensions containing xanthan gum (0.1 wt %) to improve particle dispersion and stability.^[20] The addition of xanthan gum did not alter the initial r_{1p} value of any of the hybrid materials, but its presence is important to keep the r_{1p} value nearly constant with time (Figure S3 in the Supporting Information). A fractional decrease of the relaxivity over a period of approximately one hour is easily avoided by shaking the solution.

The average size of the nanoparticles in the aqueous suspension was estimated by using a dynamic light scattering (DLS) technique. The hydrodynamic diameter was determined to be approximately 100 nm for all three hybrid materials, which suggests the presence of small aggregates of two to three nanoparticles in solution (Figure S4 in the Supporting Information).

The r_{1p} values (per Gd) measured (20 MHz and 310 K) for **1**/MCM-41, **2**/MCM-41 and **3**/MCM-41 were 26.6 ($r_{1p} \approx 9700$ per particle), 20.3 ($r_{1p} \approx 15900$ per particle) and $14.6 \text{ mM}^{-1} \text{ s}^{-1}$ ($r_{1p} \approx 3500$ per particle), respectively. The pH dependence of the relaxivity was determined in the range 3.5 to 8.4 since at lower or higher pH values the mesoporous MCM-41 silica nanoparticles became amorphous, as evidenced by XRD data (Figure S5 in the Supporting Information). Although the relaxivity only shows a limited increase for **3**/MCM-41 (+6%), in the case of the other two systems a larger increase is observed, being more pronounced for **2**/MCM-41 (+18%) than for **1**/MCM-41 (+14%) (see Figure S6 in the Supporting Information). This behaviour suggests that: 1) the integrity of the conjugated complexes is maintained over a large pH range; and 2) some electrostatic

interaction occurs between the anchored complexes **1** and **2** and the protonated groups on the silica surface.

Relative to the complexes in the monomeric form,^[1] a large relaxivity enhancement is observed (150–500%) as a consequence of the dramatic reduction of the rotational mobility of the paramagnetic units anchored to the nanoparticles.

These relaxivity values do not follow the trend expected on the basis of the properties of the monomeric complexes (q , τ_R and τ_M) and in the absence of any interaction with the silica surface: **3** ($q=2$; short τ_M) > **2** ($q=1$; short spacer; fast water-exchange rate) > **1** ($q=1$; long linker chain; long τ_M). Clearly, the chemical groups present on the surface of the functionalised particles have a strong influence on the relaxometric properties of the conjugated Gd^{III} complexes. In particular, the amino and silanol groups (ca. 6.4 Si–OH per nm²) present in large number on the silica surface are likely to be primarily involved in the modulation of the relaxivity.^[5] Electrostatic interactions are expected between the amino groups, which are protonated around neutral pH in the aqueous suspensions, and the anionic complex **2** that probably include a number of hydrogen-bonded water molecules. As a consequence, the coordinated water molecule may present an increased residence lifetime that limits the relaxivity. In the case of the GdDO3A derivatives, it is well known that one or both the coordinated water molecules can be displaced by oxygen-donor groups.^[21] Thus, it is possible to propose that the particularly low relaxivity value of **3**/MCM-41 arises from the displacement of one water molecule by an –OH group of an adjacent silanol on the surface of the nanoparticle. On the other hand, the neutral, $q=1$ complex **1** should be less sensitive to the chemical nature of the surface groups.

To get more insight into the chemical role of the support on the magnetic relaxation efficiency of the paramagnetic probes, the hybrid materials were reacted with acetic anhydride in DMF to transform the –NH₃⁺ groups into neutral amide groups (Figure 4).

IR spectra of the final solids indicated that nearly all the amino groups were acetylated (Figure S7 in the Supporting Information) because the –NH₂ peaks almost disappeared and were replaced by the bands of amide groups. This modification should have a very limited impact on the relaxomet-

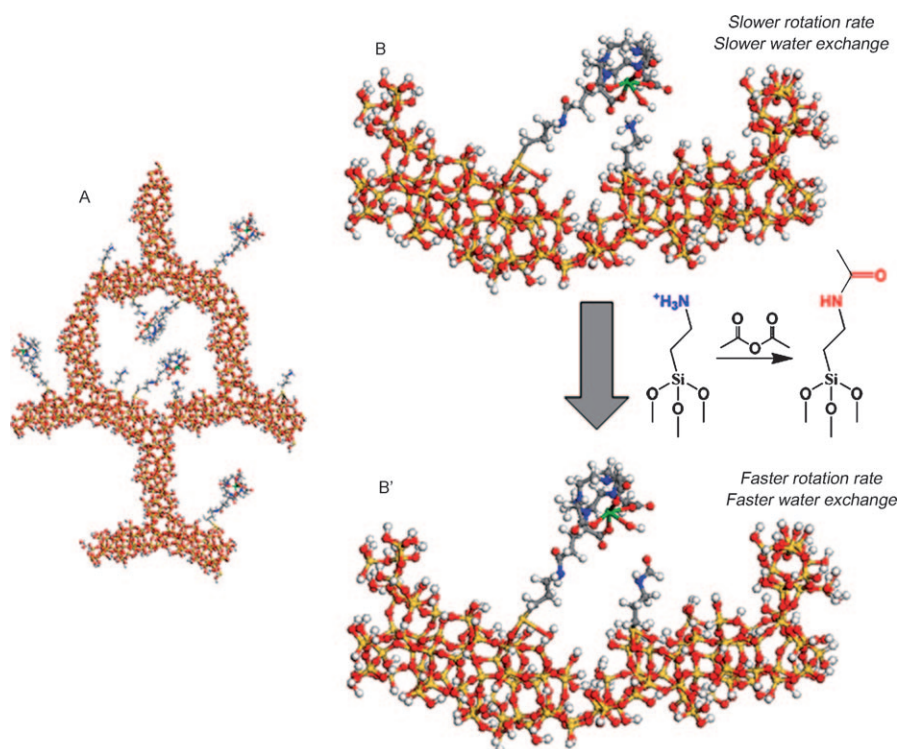


Figure 4. Schematic representation of the paramagnetic complexes grafted on mesoporous silica nanoparticles (A) and of the Gd^{III} complex/silica surface interaction before (B) and after (B') acetylation of the amino groups. (silicon: yellow; oxygen: red; hydrogen: white; nitrogen: blue; carbon: grey; gadolinium: green). The realistic model of MCM-41 was adapted by P. Ugliengo et al. in ref. [22].

ric properties of the conjugated complexes **1** and **3**, whereas the relaxivity of **2**/MCM-41 should be markedly affected.

The r_{1p} value (per Gd) measured (20 MHz and 310 K) for the acetylated **1**/MCM-41 showed a moderate increase passing from 26.6 to 30.7 mm^{−1}s^{−1}. Similarly, for **3**/MCM-41 the relaxivity only changed from 14.6 to 13.6 mm^{−1}s^{−1}. On the other hand, the transformation of protonated amino groups into neutral amide functionalities resulted in a relaxivity enhancement of 86% for **2**/MCM-41 from 20.3 to 37.8 mm^{−1}s^{−1} (Figure 5). This high r_{1p} value, coupled with the high molar amount of **2** grafted onto the silica nanoparticles results in the impressive value of relaxivity per particle of approximately 29500 mm^{−1}s^{−1}, which is relevant for future application of this hybrid material in molecular imaging procedures.

Further information was gained by measuring the magnetic-field dependence of the water proton longitudinal relaxivities for aqueous suspensions of the three materials over the frequency range 0.5–70 MHz and at 310 K (Figure 6).^[1] These nuclear magnetic relaxation dispersion (NMRD) profiles allow a detailed characterisation of the paramagnetic solutes in terms of a large set of structural and dynamic parameters. All the profiles have in common a similar shape, with a rather narrow peak centred around 30 MHz, typical of slowly tumbling systems (long τ_R). The experimental data were fitted to the Solomon–Bloembergen–Morgan equations for paramagnetic relaxation, modified by incorporating

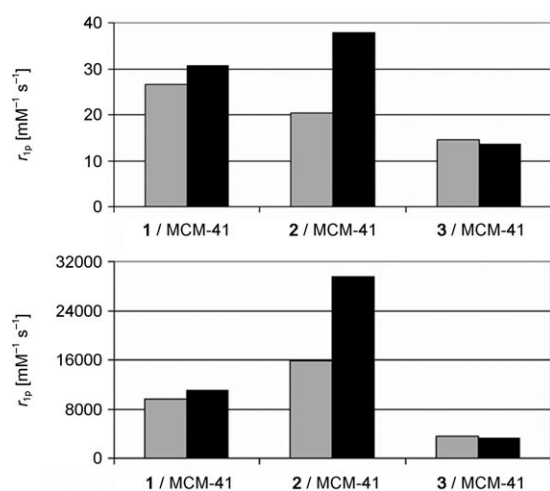


Figure 5. Plot of the relaxivity, at 20 MHz and 310 K, per Gd (top) and per particle (bottom) for the silica-conjugated complexes before (grey) and after (black) acetylation of the amino groups.

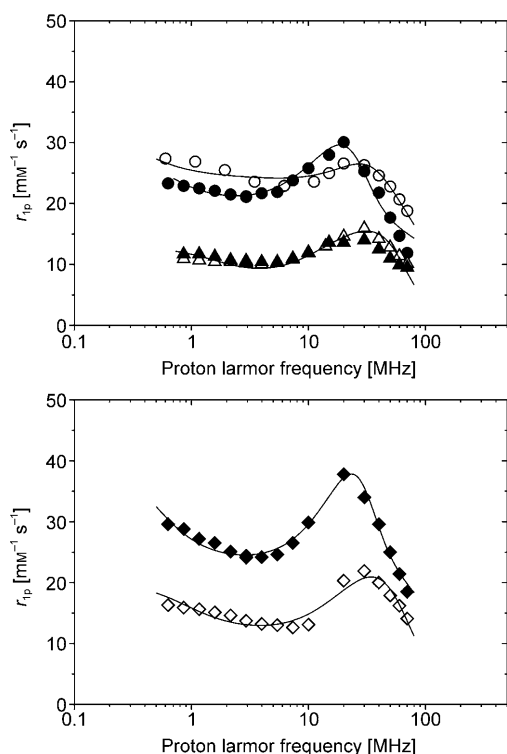


Figure 6. $1/T_1$ NMRD profiles at 310 K for **1**/MCM-41 (left, filled circles), **2**/MCM-41 (right, diamonds) and **3**/MCM-41 (left, triangles) before (\circ) and after (\bullet) acetylation of the amino groups. The best-fit curves were calculated using the parameters of Table 2.

the Lipari–Szabo description of the rotational dynamics. This approach considers the effects on the relaxation given by two types of motion: a global motion of the nanoparticles described by a reorientation correlation time, τ_{RG} , and faster local rotation of the chelate about the axis of the linker with a reorientation correlation time, τ_{RL} . The coupling of local and global motions is given in terms of the parameter S^2 :

$S^2=1$ when the local rotation of the Gd complex is impeded ($\tau_{RG}=\tau_{RL}$), and $S^2=0$ when the local motion is totally independent of the global tumbling of the nanoparticle.

In the fitting procedure the value of the parameter τ_{RG} was fixed to 100 μ s to account for the slow tumbling motion of the large particle. A very good fit of the data was obtained (Figure 6) with the parameters listed in Table 2 that

Table 2. Selected best-fit parameters^[a] obtained from the analysis of the $1/T_1$ NMRD profiles (310 K) of the Gd complexes **1–3** anchored to MCM-41.

	Complex 1		Complex 2		Complex 3 ^[d]
	(A) ^[b]	(B) ^[c]	(A) ^[b]	(B) ^[c]	
τ_{RG} [ms] ^[e]	0.1	0.1	0.1	0.1	0.1
τ_{RL} [ns]	2.4	1.2	9.2	1.3	–
τ_M [μ s]	0.48	0.44	0.70	0.25	1.1
S^2	0.5	0.4	0.6	0.4	1.0

[a] The parameters for electronic relaxation (Δ^2 , τ_V) were used as empirical fitting parameters and do not have a precise physical meaning for these macromolecular systems. The distance of the coordinated water molecule(s) from the metal ion (r_{Gd-H}) was fixed to 3.0 Å. The outer-sphere component of the relaxivity was estimated by using standard values for the distance of closest approach, a (4 Å) and the relative diffusion coefficient of solute and solvent, D (3.1×10^{-5} cm²s^{−1}). [b] Before acetylation. [c] After acetylation. [d] Parameters unchanged following acetylation. [e] The results of the NMRD fits were not sensitive to its actual value in the range of 100 ns to 1 ms.

fully support the hypotheses made. For **1**/MCM-41 the acetylation of the amino groups only had a marginal effect on τ_M and S^2 , but it induced a faster local rotation that indicated the occurrence of some interaction between the Gd chelate and the surface.

The data of **3**/MCM-41 were unchanged upon chemical modification and could be reproduced only by considering an immobilised complex ($S^2=1$) with a single metal-bound water molecule with a τ_M value of 1.1 μ s. This result strongly supports the view of a strong interaction with the surface silanols with displacement of a water molecule and decreased accessibility of the solvent to the metal centre. For **2**/MCM-41 the effects of the transformation of the amino into amide groups are quite pronounced. The absence of positively charged groups on the surface of the silica nanoparticles strongly attenuates the electrostatic interaction of the metal complex, which becomes rotationally less rigid (shorter S^2 and τ_{RL}) and more accessible to the solvent molecules (faster water exchange), as schematically shown in Figure 4B'. Finally, it is worth noting that the systems investigated are extremely complex and therefore the analysis made on the basis of a theory of paramagnetic relaxation suitable for small Gd complexes in aqueous media can only represent an approximation. However, the hypothesis made to explain the experimental data is fully supported not only by the fit of the NMRD profiles but also by the temperature dependence of the relaxivity (Figure 7). Whereas for **1**/MCM-41 and **3**/MCM-41 the behaviour is unchanged upon modification of the amino groups, for **2**/MCM-41 there is a clear change from a slow exchange (relaxivity increases with tem-

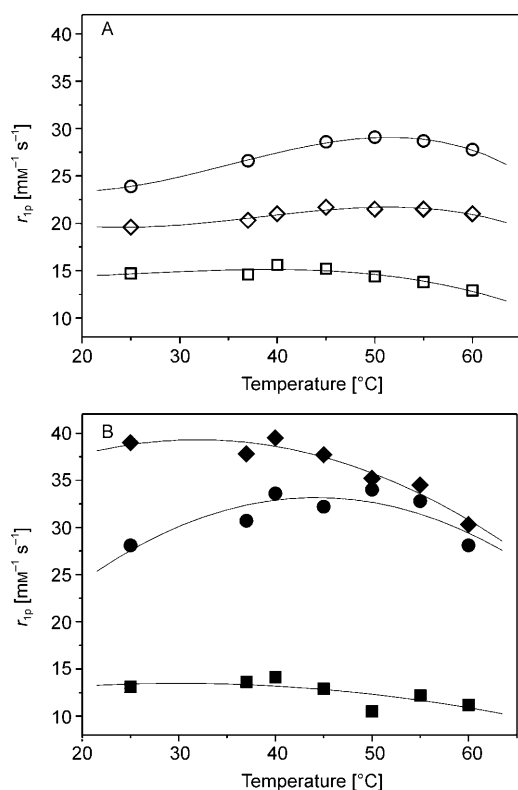


Figure 7. Temperature dependence of ^1H r_{1p} for **1**/MCM-41 (■), **2**/MCM-41 (●) and **3**/MCM-41 (◆) at 20 MHz A) before and B) after acetylation of the amino groups.

perature) to an intermediate/fast exchange regime following the acetylation of the amino groups.

Conclusion

The overall results presented here demonstrate that the type of Gd^{III} chelate and the chemical nature of the support play a key role in determining the magnetic relaxation efficiency of paramagnetically labelled mesoporous silica nanoparticles. Dramatic relaxivity enhancement and high payload were observed for a stable Gd–DOTA derivative after acetylation of the surface amino groups of the hybrid material. Analysis using nuclear magnetic resonance dispersion spectroscopy allows a detailed description of the parameters influencing the relaxivity and provides a fundamental tool for exploring further improvements.

Experimental Section

All chemicals were purchased from Sigma–Aldrich Co. and were used without purification unless otherwise stated. NMR spectra were recorded on a JEOL Eclipse Plus 400 (operating at 9.4 T). ESI mass spectra were recorded on a Waters SQD 3100.

Synthesis of the Gd^{III} complexes **1, **2** and **3**:** **L1**,^[7] **L2**^[18] and **L3**^[19] were synthesised according to the literature. For **L2** and **L3**, the literature procedures were slightly modified. In both cases the synthesis started from

DO3A(*t*BuO)₃.^[23] For **L2**, that is, DOTAGA, the secondary amino group of DO3A(*t*BuO)₃ was alkylated with (*S*)-2-bromopentanedioic acid di-*tert*-butyl ester^[24] in CH₃CN using anhydrous K₂CO₃ as base. After silica gel column chromatography, **L2** was obtained by deprotection of the *tert*-butyl esters with a solution of CH₂Cl₂ and trifluoroacetic acid (1:1). **L3** was prepared by alkylation of DO3A(*t*BuO)₃ with benzyl-6-bromohexanoate followed by hydrogenolysis of the benzyl ester and deprotection of the *tert*-butyl esters again with a solution of CH₂Cl₂ and trifluoroacetic acid (1:1).

The Gd^{III} complexes were synthesised by slowly adding an equimolar amount of GdCl₃ solution (about 120 mM in water) to a 40 mM ligand solution, maintaining the pH at 6.5 with NaOH. The mixture was allowed to stir overnight at room temperature; then the pH was raised to 8.5 and the mixture was stirred for 2 h. Centrifugation at 7000 rpm for 5 min at 10 °C allowed the separation of Gd(OH)₃ from the solution. Finally, the solvent was removed under reduced pressure leading to the formation of the desired product as a white powder. ESI-MS: *m/z* calcd for **1** (C₂₂H₃₄GdN₆O₁₀): 700.2; found: 700.5 [*M*–H⁺]; *m/z* calcd for **2** (C₁₉H₂₇GdN₄O₁₀): 628.7; found: 628.5 [*M*–H⁺]; *m/z* calcd for **3** (C₂₀H₃₁GdN₄O₈): 613.8; found: 613.6 [*M*–H⁺]. All peaks related to Gd^{III} complexes show the correct isotopic distribution.

Synthesis of mesoporous support: MCM-41 was synthesised and calcined following the procedure reported in the literature.^[14]

NH₂/MCM-41: Calcined MCM-41 (1.0 g) was firstly treated under vacuum at 250 °C for 2 h to activate the surface of the support, then the material was suspended in toluene (100 mL) under a nitrogen flow and 3-aminopropyltriethoxysilane (40 wt %) was added. The mixture was stirred at 50 °C for 20 h. The suspension was then filtered and the product was washed several times with diethyl ether to remove the unreacted silane. Finally, the sample was dried at 60 °C for 2 h. It is important to limit the water adsorption to preserve the properties of the silica surface.

General procedure for the anchoring of Gd complexes on NH₂/MCM-41: NH₂/MCM-41 (700 mg) was suspended in DMF (50 mL) for 30 min. In parallel, the Gd complex (0.500 g) containing a free carboxylic acid was dissolved in DMF (40 mL) and activated by adding one molar equivalent of *O*-(7-azabenzotriazol-1-yl)-*N,N,N',N'*-tetramethyluronium hexafluorophosphate and *N,N*-diisopropylethylamine. The solutions of the activated complexes were added to the suspension of NH₂/MCM-41 and stirred at 50 °C for 24 h. The suspensions were then filtered and the products were washed several times with H₂O to remove the unreacted complexes. We have observed for three different batches that after washing the suspended solid sample (500 mg) three times with water (200 mL), the longitudinal relaxation rate (*R*₁) of the washing water assumed a constant value of 0.40 s^{–1} (20 MHz, 298 K) that corresponds to a diamagnetic contribution only. The synthesis of the three hybrid materials has been carried out several times and the results on the Gd content were found to be reproducible within ±5 %.

Quantification of Gd loading per particle of GdL/MCM-41 hybrid materials: The determination of the Gd loading per particle was calculated by assuming a spherical shape for the particles and a density of 0.8 g cm^{–3} for the GdL/MCM-41 samples.^[25]

Characterisation of materials

The geometry optimisations have been performed with the package TURBOMOLE 5.10^[26] at the density functional theory (DFT) level, with the B-LYP functional^[27] and 6-31G* basis set^[28] for second-row atoms and Hay and Wadt pseudopotential and basis set^[29] for lanthanides.

Chemical compositions of GdL/MCM-41 hybrid materials were determined with plasma emission spectroscopy coupled to mass spectrometry (OES-MS) by NEOSIS s.a.s. Lab., Turin, Italy.

Infrared (IR) spectra of GdL/MCM-41 and the pristine porous supports have been recorded under vacuum conditions in the range 4000–400 cm^{–1} at 4 cm^{–1} resolution using a Bruker Equinox 55 spectrometer.

XRD patterns were obtained on a ARL XTRA48 diffractometer using CuK α radiation (λ = 1.54062 Å).

N₂ physisorption measurements were carried out at 77 K in the relative pressure range from 1 × 10^{–6} to 1 *P*/*P*₀ by using a Quantachrome Autosorb 1MP/TCD instrument. Prior to the analysis the samples were out-

gassed at 373 K for 3 h (residual pressure lower than 10^{-6} torr). Apparent surface areas were determined by using the BET equation, in the relative pressure range from 0.01 to 0.1 P/P_0 . Pore volume and diameter were defined by the Barret–Joyner–Halenda (BJH) approach (applied to the desorption branch).

Thermogravimetric analyses (TGA/DTG) of materials were performed under an oxygen flow (100 mL min^{-1}) with a SETSYS Evolution TGA-DTA/DSC thermobalance, heating from 50 to 1200°C at $10^\circ\text{C min}^{-1}$ (see Figure S2 in the Supporting Information).

DLS experiments were carried out by using a Zetasizer NanoZS, Malvern, UK, operating in a particle size range from 0.6 nm to $6 \mu\text{m}$ and equipped with a He-Ne laser with $\lambda = 633 \text{ nm}$. The samples were dispersed in water in the presence of xanthan gum (0.1 wt %) to improve particle dispersion. Before the measurement, the suspensions were sonicated for 30 min. The particles dispersed in water tend to form large aggregates that eventually precipitate. In the solution stabilised with xanthan gum this effect is strongly limited and no precipitation is observed after days (Figure S3 in the Supporting Information).

The water proton longitudinal relaxation rates of diluted aqueous suspensions of hybrid materials 1/MCM-41, 2/MCM-41 and 3/MCM-41 in the presence of xanthan gum (0.1 wt %) were measured by using a Stellar Spinmaster spectrometer (Mede, Italy) operating at 0.5 T and 298 K. The amount of Gd^{III} in the final materials was estimated by ICP-OES (NEOSIS s.a.s. Lab, Turin, Italy). For the measurement of the relaxation rates, the standard inversion-recovery method was employed (16 experiments, 2 scans) with a typical 90° pulse width of 3.5 ms, and the reproducibility of the T_1 data was $\pm 0.5\%$. The temperature was controlled with a Stellar VTC-91 airflow heater equipped with a copper-constantan thermocouple (uncertainty of $\pm 0.1^\circ\text{C}$). The proton $1/T_1$ NMRD profiles were measured on a fast field cycling Stellar SmarTracer relaxometer over a continuum of magnetic field strengths from 0.00024 to 0.25 T (corresponding to 0.01–10 MHz proton Larmor frequencies). The relaxometer operates under computer control with an absolute uncertainty in $1/T_1$ of $\pm 1\%$. Additional data points in the range 15–70 MHz were obtained on the Stellar Spinmaster spectrometer. The collection of these latter data is more time consuming and some precautions need to be taken. Over a period of one hour, we observed about 8% decrease of relaxivity due to a slight instability of the suspension (Figure S3 in the Supporting Information). Therefore, the sample tube was shaken using a vortex mixer for 0.5–1 min before each measurement.

Acknowledgements

The authors acknowledge financial support from Regione Piemonte (Nano-IGT and NANOLED projects) and thank Dr. Filip Kielar (DISAV-Alessandria) for his technical support during the synthesis of complex 2.

- [1] P. Caravan, J. J. Ellison, T. J. McMurphy, R. B. Lauffer, *Chem. Rev.* **1999**, 99, 2293–2352; S. Aime, M. Botta, E. Terreno, *Adv. Inorg. Chem.* **2005**, 57, 173–237; C. F. G. C. Galdes, S. Laurent, *Contrast Media Mol. Imaging* **2009**, 4, 1–23; J. Gao, H. Gu, B. Xu, *Acc. Chem. Res.* **2009**, 42, 1097–1107.
- [2] S. Aime, S. Geninatti Crich, E. Gianolio, G. B. Giovenzana, L. Tei, E. Terreno, *Coord. Chem. Rev.* **2006**, 250, 1562–1579; S. Aime, D. Delli Castelli, S. Geninatti Crich, E. Gianolio, E. Terreno, *Acc. Chem. Res.* **2009**, 42, 822–831.
- [3] D. Delli Castelli, E. Gianolio, S. Geninatti Crich, E. Terreno, S. Aime, *Coord. Chem. Rev.* **2008**, 252, 2424–2443.
- [4] J. M. Hooker, A. Datta, M. Botta, K. N. Raymond, M. B. Francis, *Nano Lett.* **2007**, 7, 2207–2210; A. Datta, J. M. Hooker, M. Botta, M. B. Francis, S. Aime, K. N. Raymond, *J. Am. Chem. Soc.* **2008**, 130, 2546–2552.
- [5] M. Tsotsalas, M. Busby, E. Gianolio, S. Aime, L. De Cola, *Chem. Mater.* **2008**, 20, 5888–5893.
- [6] L. Moriggi, C. Cannizzo, E. Dumas, C. R. Mayer, A. Ulianov, L. Helm, *J. Am. Chem. Soc.* **2009**, 131, 10828–10829; C. Alric, J. Taleb, G. Le Duc, C. Mandon, C. Billotey, A. Le Meur-Herland, T. Brochard, F. Vocanson, M. Janier, P. Perriat, S. Roux, O. Tillement, *J. Am. Chem. Soc.* **2008**, 130, 5908–5915.
- [7] F. Carniato, L. Tei, W. Dastur, L. Marchese, M. Botta, *Chem. Commun.* **2009**, 1246–1248.
- [8] W. J. Rieter, J. S. Kim, K. M. L. Taylor, H. An, W. Lin, T. Tarrant, W. Lin, *Angew. Chem.* **2007**, 119, 3754–3756; *Angew. Chem. Int. Ed.* **2007**, 46, 3680–3682; M. D. Rowe, C.-C. Chang, D. H. Thamm, S. L. Kraft, J. F. Harmon, A. P. Vogt, B. S. Sumerlin, S. G. Boyes, *Langmuir* **2009**, 25, 9487–9499.
- [9] I. Rehor, V. Kubicek, J. Kotek, P. Hermann, I. Lukes, J. Szakova, L. V. Elst, R. N. Muller, J. A. Peters, *J. Mater. Chem.* **2009**, 19, 1494–1500; P. J. Endres, T. Paunesku, S. Vogt, T. J. Meade, G. E. Woloschak, *J. Am. Chem. Soc.* **2007**, 129, 15760–15761.
- [10] J. Kim, Y. Piao, T. Hyeon, *Chem. Soc. Rev.* **2009**, 38, 372–390.
- [11] K. M. L. Taylor, J. S. Kim, W. J. Rieter, H. An, W. Lin, W. Lin, *J. Am. Chem. Soc.* **2008**, 130, 2154–2155.
- [12] C. P. Tsai, Y. Hung, Y. H. Chou, D. M. Huang, J. K. Hsiao, C. Chang, Y. C. Chen, C. Y. Mou, *Small* **2008**, 4, 186–191.
- [13] J. Kim, H. S. Kim, N. Lee, T. Kim, H. Kim, T. Yu, I. C. Song, W. K. Moon, T. Hyeon, *Angew. Chem.* **2008**, 120, 8566–8569; *Angew. Chem. Int. Ed.* **2008**, 47, 8438–8441.
- [14] K. Suzuki, K. Ikari, H. Imai, *J. Am. Chem. Soc.* **2004**, 126, 462–463.
- [15] L. Tei, G. Gugliotta, Z. Baranyai, M. Botta, *Dalton Trans.* **2009**, 9712–9714.
- [16] S. Aime, M. Botta, G. Ermondi, E. Terreno, P. L. Anelli, F. Fedeli, F. Uggeri, *Inorg. Chem.* **1996**, 35, 2726–2736.
- [17] E. Terreno, P. Boniforte, M. Botta, F. Fedeli, L. Milone, A. Mortillaro, S. Aime, *Eur. J. Inorg. Chem.* **2003**, 3530–3533.
- [18] K. P. Eisenwiener, P. Powell, H. R. Maecke, *Bioorg. Med. Chem. Lett.* **2000**, 10, 2133–2135; S. G. Levy, V. Jacques, K. Li Zhou, S. Kalogeropoulos, K. Schumacher, J. C. Amedio, J. E. Scherer, S. R. Witowski, R. Lombardy, K. Koppetsch, *Org. Process Res. Dev.* **2009**, 13, 535–542.
- [19] R. T. Dean and R. W. Weber, US Patent 5053503, **1991**.
- [20] K. J. Balkus, Jr., J. Shi, *Langmuir* **1996**, 12, 6277–6281.
- [21] S. Aime, M. Botta, J. I. Bruce, V. Mainero, D. Parker, E. Terreno, *Chem. Commun.* **2001**, 115–116.
- [22] P. Uglieri, M. Sodupe, F. Musso, I. J. Bush, R. Orlando, R. Dovesi, *Adv. Mater.* **2008**, 20, 4579–4583.
- [23] D. A. Moore, *Org. Synth.* **2008**, 85, 10–14.
- [24] M. Woods, S. Aime, M. Botta, J. A. K. Howard, J. M. Moloney, D. Parker, M. Navet, M. Port, O. Rousseaux, *J. Am. Chem. Soc.* **2000**, 122, 9781–9792.
- [25] K. J. Edler, P. A. Reynolds, J. W. White, D. Cookson, *J. Chem. Soc. Faraday Trans.* **1997**, 93, 199–202.
- [26] R. Ahlrichs, M. Bar, M. Haser, H. Horn, C. Kolmel, *Chem. Phys. Lett.* **1989**, 162, 165–169.
- [27] A. D. Becke, *Phys. Rev. A* **1988**, 38, 3098–3100; C. Lee, W. Yang, R. G. Parr, *Phys. Rev. B* **1988**, 37, 785–789.
- [28] P. C. Hariharan, J. A. Pople, *Theor. Chim. Acta* **1973**, 28, 213–222.
- [29] P. J. Hay, W. R. Wadt, *J. Chem. Phys.* **1985**, 82, 270–283; W. R. Wadt, P. J. Hay, *J. Chem. Phys.* **1985**, 82, 284–298; P. J. Hay, W. R. Wadt, *J. Chem. Phys.* **1985**, 82, 299–310.

Received: February 25, 2010
Published online: July 28, 2010